

UDK: 666.3.019; 551.243.1; 666.3-127

Intergranular Space, Specific Surface Area, Grain Size Distribution and Distribution of Macro, Meso and Micropores of Multiphase Microstructure in Active Microalloyed Multifunctional Ceramics

Jelena M. Purenović^{1*)}, Milovan M. Purenović²

¹Faculty of Technical Sciences Čačak, University of Kragujevac, Serbia

²Faculty of Sciences and Mathematics, University of Niš, Serbia; Academician of Serbian Academy of inventors and scientists, Serbia

Abstract:

As a complex multiphase heterogeneous system in solid state, multifunctional active microalloyed alumo-silicate ceramics has an inhomogeneous structure with intergranular space, which is reflected in a number of structurally sensitive properties. A very complex intergranular space and numerous interactions between individual phases and grains create new boundaries and an even more complex space with much smaller micrograins, which are formed by grain fragmentation by dislocations displacement. In addition to reducing macro and meso porosity, densification of intergranular space increases the number of micro pores. Intergranular surface area and volume are considered as dislocation space. Quantitative metallography method was applied to determine grain size distribution using software for automatic analysis. Specific surface tests and pore distribution were performed on special samples of multifunctional ceramics. Standard methods for determining specific surface area of samples in vacuum were used. Obtained results, which were relevant in terms of theoretical and practical implications, confirmed that multifunctional active microalloyed ceramics had a developed surface with significant number of meso and micro pores. Due to constancy of grain fragmentation process, there were significant changes in micromorphology and all multifunctional properties, as well as movement of dislocations, which made a significant contribution to contemporary research in this field.

Keywords: Multifunctional ceramics; Grain distribution; Macro, meso and micro porosity; Dislocations; Fragmentation.

1. Introduction

Recently, microalloying has become an important technique which is applied to micro and nanostructured materials. Microalloying implies the addition of individual elements in small (ppm) quantities, while the modified structure is characterized by specific for results in significant changes in the values of electrical conductivity and electrode potential. Microalloyed and structurally modified solid materials have high porosity (30%), with macro, meso and micro pores. The heterogeneous structure of these composite materials has confirmed a direct connection between porosity and structure, especially when it comes to nanostructured fragmented crystals. M. M Purenović et al. [1-9], synthesized ceramic microalloyed and nanostructured materials based on alumo-silicate ceramics. Exceptional

*) **Corresponding author:** jelena.purenovic@gmail.com (Dr. Jelena Purenović)

results were obtained for porous ceramic materials with 30% porosity and nanostructured fragmented crystals, in terms of their electrochemical behavior in contact with water containing arsenic. Alloying of alumo-silicate matrix with Mg and microalloying with Al resulted in obtaining a very useful multifunctional material. The microstructure had an amorphous-crystalline structure with a modified kaolinite-bentonite matrix with respect to nonstoichiometric composition of magnesium-silicate and alumo-silicate amorphous and crystalline layers. This composite multifunctional material had microstructure and morphology that supported changes in numerous structurally-sensitive properties. Due to the presence of dissolved hydrogen in solid state and its molecularization, the whole composite was in a very mechanically stressed state of high potential energy, which could affect the appearance and significantly increase the dislocations and point defects. Thus, due to exceeding the stress limits in certain areas and grains of the matrix, it could cause the initiation of dislocations and spontaneous fragmentation of macro and micro grains into even smaller submicro grains and mosaic blocks.

One of the key works [10], from the very beginning of research and physico-chemical characterization of microalloyed and alloyed ceramics, referred to obtaining alumo-silicate ceramics modified with magnesium and microalloyed with aluminum in order to study the physical and microstructural properties of such obtained composite multifunctional material. Ceramics with such active additives did not significantly change the macro morphology and structure, but resulted in micro amorphization of the crystal grain surface. Consequently, a thin layer of amorphous magnesium and aluminum silicates was formed on the grain surface. The porous macrostructure of ceramics, together with macro, meso and micro pores formed a developed surface which was responsible for surface activity and surface states of different energy levels. Examination of microstructure of sintered samples was performed using a scanning electron microscope (SEM), equipped with energy dispersive spectrometer (EDS).

Unconventional multifunctional materials could be classified as modern ceramic materials with predicted properties which define chemical composition and structure of ceramic material. The structure of this material is specifically arranged so that it has very high porosity, 25-30%, with a multitude of macro, meso and micro pores, and a developed specific surface. Modified alumo-silicate ceramics represent an extremely important group of oxide composite ceramics, characterized by an amorphous-crystalline structure. The amorphized structure of ceramics, with finely distributed crystal regions, enables numerous redox processes in interaction with water and aqueous electrolyte solution. Depositing the exchanged mass in the existing pores results in the changes in structure and morphology, and continues to cause even greater activity and more drastic changes in the morphology and structure of secondary phases of deposited substances originating from water.

Porous solids, including porous ceramics, have a specific function in heterogeneous solid-water systems, due to the very complex transport and diffusion phenomena associated with macro and micro pores. Regardless of their dimensions, the pores, are defined spaces where mass can be exchanged, either during thermal processes, i.e. sintering, when the corresponding phases of non-stoichiometric composition are separated on the pore walls, or when interacting in the system with model water (distilled water to which the corresponding salts have been added in a given concentration) when there is a deposition or precipitation of certain ingredients from the water on the surface. The pores in kaolinite-bentonite ceramics activated with Mg are formed by appropriate thermal processes at elevated temperatures, during which the gas phase develops. Simultaneous addition of some microalloying additives and Mg in the form of salt and sintering at elevated temperatures leads to the separation of Al and Mg excess outside the stoichiometric composition of Mg and Al silicates. The obtained ceramics are porous, microalloyed and with silicate structures of nonstoichiometric composition. Excess of these and some other metals causes great physical and chemical activity on the surfaces of the solid phase, especially on the inner surfaces of the pores.

Therefore, by adding active components above the stoichiometric composition, very active absorption centers are created, centers for the redox process-electrochemical centers, i.e. microgalvanic couplings and unstable phases that are chemically active and when interacting with water dissolve to give the corresponding cations and anions. Due to the possibility of numerous processes on microalloyed Mg-Al-silicate ceramics, redox processes being dominant, i.e. oxidation process takes place at one end and the reduction process at the other end, this ceramic is a powerful tool for purifying drinking and wastewater from harmful impurities of heavy metal cations, such as Mn, Fe, As, Cr, Ni, etc., as well as other ions and radicals present in the treated water [11].

2. Materials and Experimental Procedures

2.1 SEM analysis of multifunctional ceramics

Microphotographs were taken by SEM model JEOL JSM-5300, which allowed samples to be observed at magnifications up to 50.000x, with the ability to achieve high resolution of 4.5 nm and spot details of the microstructure. Therefore, the micro morphology of the samples was observed. In addition to average grain and pore size and distribution as microstructural constituents of ceramics material, microstructural analysis method enabled observing the basic details of microstructural changes during sintering [24,25].

Firstly, microphotographs of the initial (pure) powder of the alumo-silicate matrix were taken (Fig. 1). The particle size was not uniform and ranged from 10-50 μ m. The particles had irregular polygonal shape, with an amorphous grain boundary.

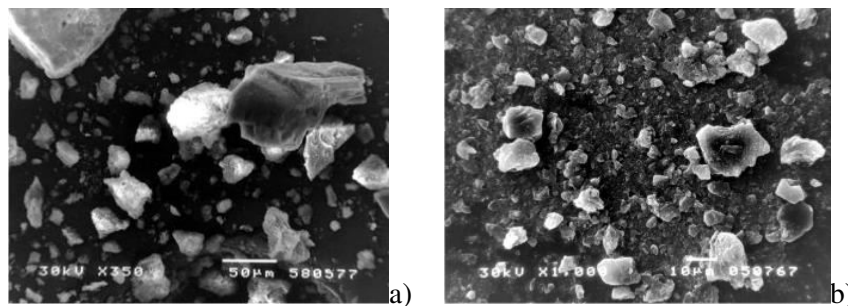


Fig. 1. SEM microphotographs of pure alumo-silicate matrix powder: a) magnification 350x, b) magnification 1.000x.

Fig. 2 showed the powder of the alumo-silicate matrix mixed with the powder of active additives. The grains with amorphous boundary of different sizes (from smaller to extremely large) were observed.

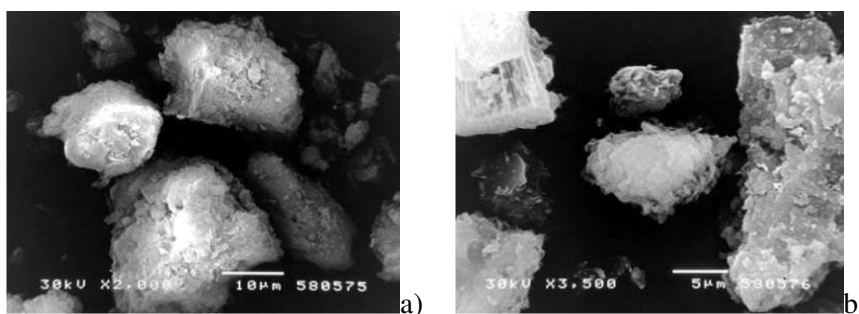


Fig. 2. SEM microphotographs of alumo-silicate matrix powders and additives mixtures: a) magnification 2.000x, b) magnification 3.500x.

SEM microphotographs of the primary microstructure of active microalloyed ceramics, (Fig. 3), showed a very complex, non-uniform and extremely porous structure.

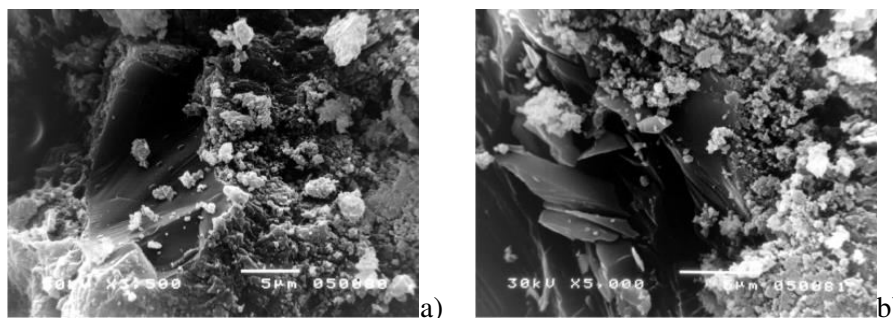


Fig. 3. SEM micrographs of primary microstructure of active microalloyed ceramics with 6 wt.% additive: a) magnification 3.500x, b) magnification 5.000x.

Non-uniformity was reflected in differences in grain size (1-20 μm), micromorphology, porosity and amorphous-crystalline micromorphology. Microphotographs showed a layered structure with aggregates in the form of plate particles of different dimensions, which originated from bentonite. In addition to amorphous regions and coarse-grained microstructure, highly crystalline grains were also present, especially in samples with 6 wt.% additive. A layered structure with polygonal grain shapes was present, and planar surface defects were present in some grains. In general, active ceramics was characterized by multiphase amorphous-crystalline structure and morphology, with the inevitable nonstoichiometry of individual phases in a complex multiphase system of microalloyed ceramics. Most likely, the crystalline phases were imprinted in the porous amorphous mass of the alumo-silicate matrix and microalloying and alloying additives, i.e. the crystalline phases were masked by the amorphous phase that enveloped each grain. The existing multiphase, with highly developed crystal blocks housed in an amorphous silicate matrix, Mg and Al, was reflected in surface textures and complex interfacial boundaries. Some areas had a large volume of small layers, formed by layering, which were very close to each other and thus created compact layers of microstructure, while others had leaves with very open pores [12]. Thus, after modification of the matrix, fragmentation of crystal grains, partial deformation in the form of dendrites with a fractal nature and amorphization of alumo-silicates occurred. On the other hand, particles of microalloying and alloying additives were present on the surface of the matrix in the form of clusters of thin micro and nano metallic films, or were present as separate phases deposited on the alumo-silicate matrix in the form of silicate or oxide. It was noticed that the grains, which were of different shapes, were coated with a thin layer of metal films, silicates and oxides of aluminum and magnesium.

SEM microphotographs showed the microstructure of microalloyed alumo-silicate ceramics at various magnifications, ranging from 350x (Fig. 1a) to 5.000x (Fig. 3b). At higher magnifications, a specific porous microstructure was clearly observed, formed by the penetration of molten aluminum and magnesium into the alumo-silicate matrix and metallized areas. The areas seen in the microphotograph as a brighter surface were actually microstructural areas, modified by deposited aluminum, which melted at the sintering temperature, and liquid aluminum infiltrated the pores and intergranular space, where there was a possibility of reaction with added magnesium, which represented an alloying component. The result was a layered curved structure, with macro and meso pores of different shapes and wide range of sizes. The shape of the pore opening was mostly in the form of incisions and ellipses, and less often spherical. SEM microphotographs unequivocally indicated that alumo-silicate ceramics, as a dielectric material, was in fact metallized by

discrete-cluster distribution of aluminum and magnesium accumulations, as well as by the formation of metal films in the intergranular space.

2.2 EDS analysis of multifunctional ceramics

EDS characterization of microalloyed alumo-silicate ceramics was performed immediately after SEM analysis, thus obtaining a qualitative composition by identifying the appropriate peaks. The EDS model used to make the diagrams was LINK QX 2000 analytical. EDS spectra, with accompanying microphotographs, provided information on the composition of active microalloyed ceramics, indicating a large number of oxides present.

As shown in Fig. 4, in addition to oxides of Mg, Al and Si, oxides of other elements were present, i.e. Na, K, Ca, Ti and Fe, which originated from the natural alumo-silicate matrix. The dominant peak was observed for silicon, which originated from silicon tetrahedral layers of alumo-silicate matrix, and also occurred due to the presence of crystalline phases of quartz and cristobalite, as well as the always present amorphous silicate phases of alkali and alkaline earth metals. Judging by the height and width of individual peaks, it was obvious that oxides of Si, Al and Mg were dominant, which was expected. On the other hand, other present oxides and elements had impurity status. Due to the pronounced peaks of Al and Mg, the above EDS diagram with accompanying SEM microphotography confirmed that these additives had been implanted into the structure of microalloyed ceramics. These peaks unequivocally confirmed that there was an implantation, i.e. the installation of microalloying and alloying elements in the structure of the solid phase of ceramics.

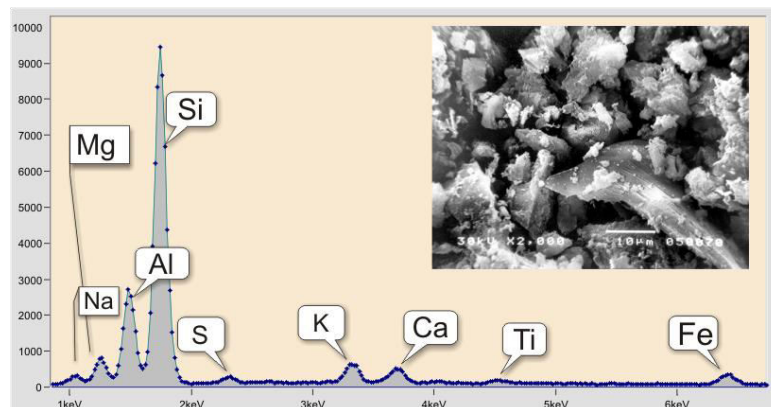


Fig. 4. EDS diagram of primary microstructure of active microalloyed ceramics with 6-wt.% additive.

2.3 The analysis of multifunctional ceramics quantitative metallography results

The method of quantitative metallography enabled the determination of the grain size distribution present in the samples. Using the software for automatic microphotography analysis, SemAfore 4, the grain size (minimum, maximum and mean values) was determined, as well as the grain size distribution. This method was performed on a large number of microphotographs of active microalloyed ceramics of primary and primary-secondary microstructure, where at least 150 grains were observed for each sample, located at different places of the same sample. Thus, the relative quantitative grain size distribution was acquired, as shown by the obtained histograms and the summary cumulative distribution curve.

This method of quantitative metallography using SEM microphotographs and SemAfore 4 software showed that the pure powder of alumo-silicate matrix had a mean grain

size of 10 μm . There were also smaller grains, as well as several larger agglomerates, up to several tens of micrometers (Fig. 5). However, after the sintering process, the grain size decreased drastically, as expected, due to modifications and complex interactions in microalloyed ceramics. Adequate curves from the grain size distribution of microalloyed ceramics, shown in Fig. 6, verified that higher percentage of grains (about 30%) were up to 4 μm , while smaller percentage of grains were up to 15 μm , and some agglomerated grains reach sizes up to 30 μm [13-15].

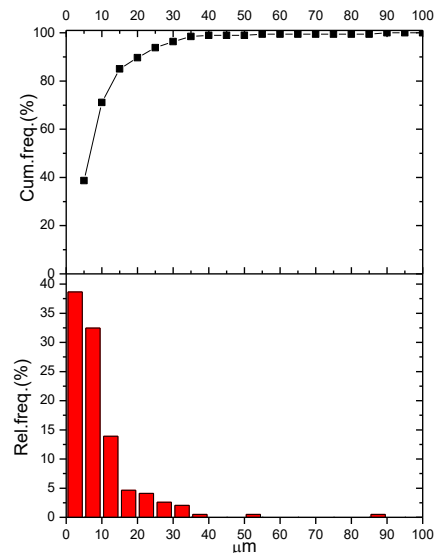


Fig. 5. Grain size distribution for pure alumo-silicate matrix powder: a) cumulative frequency (up); b) relative frequency (down).

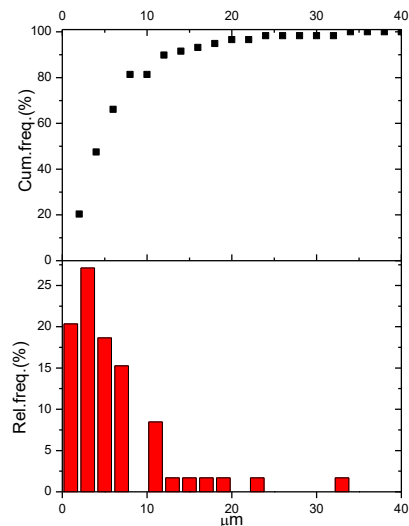


Fig. 6. Grain size distribution of active microalloyed ceramics with 6 wt.% additive: a) cumulative frequency (up); b) relative frequency (down).

Cumulative curves illustrated inhomogeneous grain size distribution. Also, it was noticed that the sintering process caused a decrease in grain size, which was a consequence of grain fragmentation in the process of synthesis and sintering, by initiating dislocations accumulated at phase boundaries and grain boundaries, due to thermal decomposition of

additives and gas phases in pores and capillaries. Consequently, a large number of fragmented mosaic blocks and smaller grains were present in the structure of active microalloyed ceramics. The process of grain fragmentation confirmed that there were numerous interactions of present phases and impurities in the intergranular space, where fragmentation took place due to redistribution and accumulation of dislocations, which contributed to further fragmentation of larger macro grains into micro grains, and the micro grains were translated into an almost amorphous state with a fractal nature.

2.4 Review and analysis of specific surface testing original results and multifunctional ceramics pore dimensions distribution

Specific surface tests and pore distributions were performed on Sorptomatic 1990 instrument (Thermo Fisher Scientific, USA). The method of sample preparation for analysis was reduced to degassing the defined sample mass at a temperature of 150°C for 18h, with a program. The tests were performed on samples of active microalloyed ceramics with 6 wt%.

Experimental operating parameters, which included working conditions on the instrument and the basics for graphs constructing, were presented. Firstly, the standard adsorption-desorption curve with mild hysteresis was demonstrated. Then, graphical representation obtained by applying characteristic models, which implied that after the application of data from basic adsorption-desorption curve which was the only curve recorded, derivative data were used in other to determine the required size by means of appropriate theoretical approach. In this way, the following sizes were determined: adsorption monolayer volume, monolayer content, total material surface area, mean pore diameter, maximum pore diameter, total pore volume, total pore area, monolayer volume, monolayer capacity (volume), micro pores volume, and mezzo pores surface. The following models were used in the paper: Bruner, Emet and Teler method, Barrett, Joyner and Halenda method, Dollimore and Heal method, Dubinin and Raduskevich method, Lippens and de Boer method, and Sing method.

A standard method was applied to determine the specific surface area of the dried sample in vacuum, using the process of adsorption and desorption of nitrogen at temperatures of 77 K. The obtained isotherm was shown in Fig. 7.

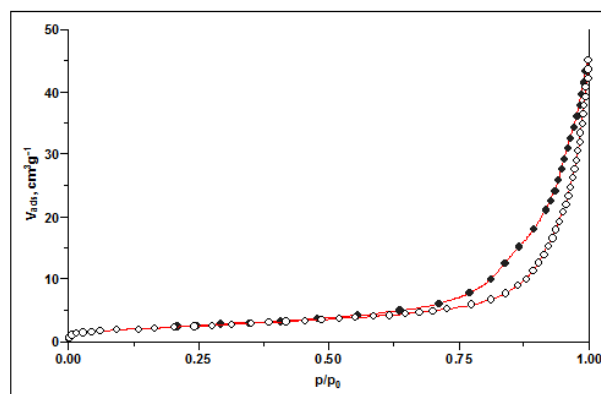


Fig. 7. Adsorption isotherm of active microalloyed ceramics.

As seen on the diagram in Fig. 7, at p/p_0 ratios less than 0.7, the adsorption-desorption processes of nitrogen were completely reversible and showed a relatively small amount of adsorbed and desorbed nitrogen. However, at p/p_0 ratios greater than 0.7, hysteresis occurred between adsorption and desorption processes, with an exponential increase in the volume of

adsorbed nitrogen per unit mass of active ceramic. The pore volume according to Gurvich, at a p/p_0 ratio of 0.999 was $0.0697 \text{ cm}^3/\text{g}$, while at a p/p_0 ratio of 0.98 the pore volume was $0.0479 \text{ cm}^3/\text{g}$.

During further research of specific surface and active microalloyed ceramics monolayer volume, an isotherm based on the dependence of $P/V_{\text{ads}}(p^0-p)$ on relative pressure (p/p^0) was obtained using B.E.T. method with two parameters, which was shown in Fig. 8. The results of individual parameters were shown in Table I.

Tab. I Working conditions and results obtained by Bruner, Emet and Teler method with two parameters.

| Working conditions | Value |
|---|-----------------------------|
| Linear regression p/p_0 | 0.069 - 0.296 |
| Alignment | $0.00832439 \pm 0.00037562$ |
| Slope | $0.49460841 \pm 0.00192021$ |
| r^2 | 0.99996986 |
| Results | |
| Monolayer volume / $\text{cm}^3 \text{ g}^{-1}$ | 1.9883 |
| Monolayer content / mmol g^{-1} | 0.0887 |
| Specific surface / $\text{m}^2 \text{ g}^{-1}$ | 8.6545 |

Having in mind the diagram in Fig. 8 and the results in Table I, with linear regression $p/p^0=0,069-0,296$, the given values for comparison-slope, correlation coefficient $r^2=0,999999$, specific area 8, 6545 and monolayer volume 1, 9883, a very high value of volume and quantity of monolayer was achieved. Regarding the diagram in Fig. 8, an area with linearity was reached (full circles), as well as partial deviation from linearity, which was defined by empty circles.

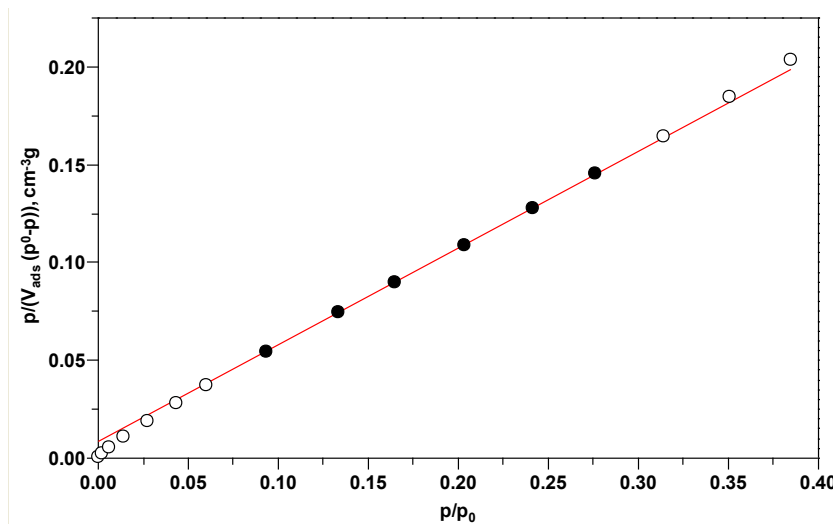


Fig. 8. Specific surface area and active microalloyed ceramics monolayer volume determined by B.E.T. method with two parameters.

Further specific area research was continued by B.E.T. method with three parameters. The method was based on showing the dependence of V_{ads} on relative pressure, as shown in Fig. 9 and Table II.

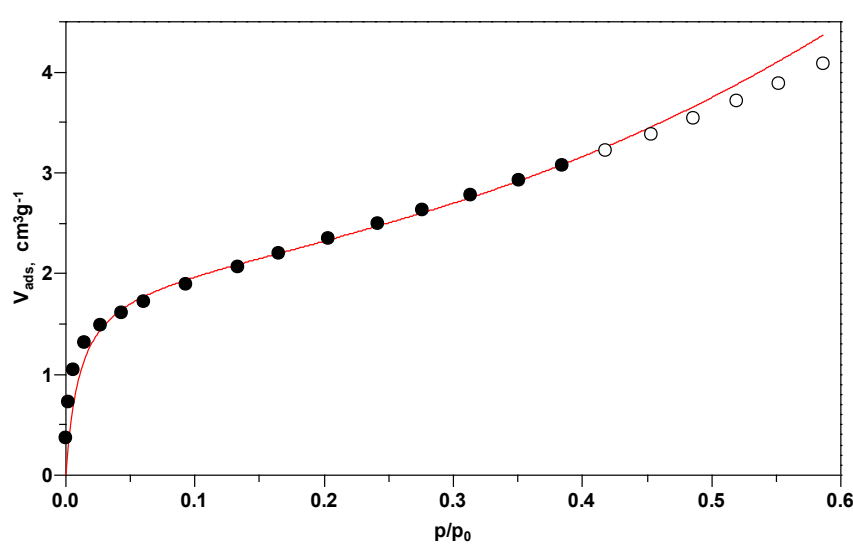


Fig. 9. Specific surface area and active microalloyed ceramics monolayer volume determined by B.E.T. method with three parameters.

Tab. II Working conditions and results obtained by B.E.T. method with three parameters.

| Working conditions | Value |
|--|----------------|
| Simplex fitting p/p_0 | 0.0001 - 0.401 |
| r^2 | 0.99626925 |
| Results | |
| Monolayer volume / $\text{cm}^3 \text{g}^{-1}$ | 1.9357 |
| Monolayer amount / mmol g^{-1} | 0.0864 |
| Specific surface / $\text{m}^2 \text{g}^{-1}$ | 8.4255 |
| C | 96.211 |
| N | 7.4486 |

Thus, after simplex fitting in the interval of relative pressure p/p_0 0.0001 - 0.401 and with a slightly lower correlation coefficient r^2 , a slightly smaller volume of monolayer and specific surface area was obtained compared to the previous method with two parameters. Starting from the fact that developed surface of active microalloyed ceramics was inevitably accompanied by pores present in intergranular space, it was crucial to determine dimensions and distribution of pores, regardless of whether they were meso, micro and submicro pores, as they were not thoroughly addressed in the literature. Due to very small diameter and high capillary pressure in submicro pores, as shown by the Kelvin equation:

$$\ln p/p^0 = \frac{2\gamma V_m}{rRT}$$

the reproductive method for determining the volume and distribution of these pores had not yet been determined. The primary focus was on the examination of meso porosity and distribution in active microalloyed ceramics. Using B.J.H. method, the mesopores of active microalloyed ceramics were tested. The graphical representation of pore volume dependence and distribution was shown in Fig. 10, and the obtained results were indicated in Table III.

As can be seen in Table III, with a linear regression of p/p_0 in the range 0.35 - 0.968, liquid nitrogen density of 0.8086 g cm^{-3} and a surface tension of $8.85 \text{ Dyne cm}^{-1}$, as very

important parameters for the Kelvin equation, appropriate results were obtained. Under these conditions, a mean pore diameter of 20.297 nm, a maximum pore diameter of 12.16 nm, a total pore volume of $0.0525 \text{ cm}^3 \text{ g}^{-1}$ and a total pore area of $12.83 \text{ m}^2 \text{ g}^{-1}$ were obtained. When comparing the value of total pore area with the obtained specific surface area of active microalloyed ceramics, it could be concluded that the dominant share in the specific surface area was occupied by the pores. Additionally, due to capillary condensation, regardless of the degree of drying of the sample, there was a sorption of water molecules from the atmosphere and a certain degree of surface coverage by this medium.

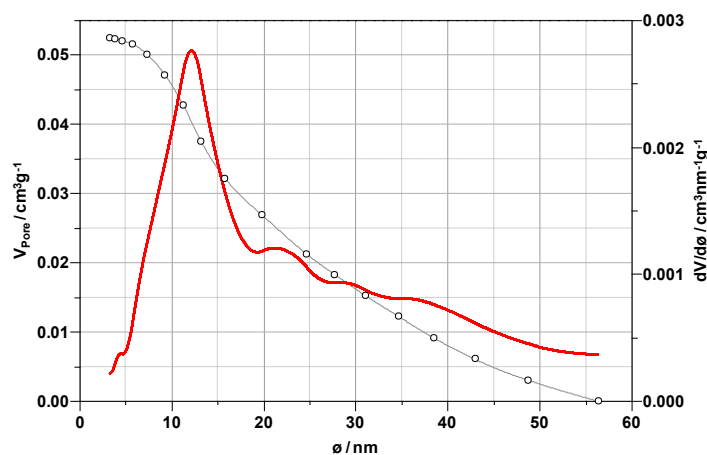


Fig. 10. Active microalloyed ceramics meso pores volume determined by B.J.H. method.

Tab. III Working conditions and pores examination results obtained by Barrett, Joyner i Halenda methods.

| Working conditions | Value |
|--|--------------|
| Linear regression p/p_0 | 0.35 - 0.968 |
| Liquid density / g cm^{-3} | 0.8086 |
| Surface voltage / Dyne cm^{-1} | 8.85 |
| Results | |
| Mean pore diameter / nm | 20.297 |
| Maximum pore diameter / nm | 12.16 |
| Total pore volume / $\text{cm}^3 \text{ g}^{-1}$ | 0.0525 |
| Total pore area / $\text{m}^2 \text{ g}^{-1}$ | 12.63 |

In addition to use of successive methods with one, two and three parameters for determining specific surface of active microalloyed ceramics, successive determination of pore volume and their distribution was performed, applying contemporary methods. Using Dollimore and Heal methods, dependence of pore volume on their diameter was determined, and corresponding results were shown in the diagram in Fig. 11, and experimental conditions and obtained results in Table IV.

The obtained results and the diagram confirmed that the values of mean and maximum pore diameters were slightly larger than those obtained by the B.J.H. method, but a significantly larger maximum pore diameter, i.e. 22.128 nm was obtained. In order to characterize the active microalloyed ceramics in a more comprehensive manner, analysis of microporosity and specific surface was performed using the methods of Dubinin and Radushkevich, Lipens and de Boer and Sing method. Combined results of these methods were shown in the diagram given in Fig. 12 and Table V; Fig. 13 and Table VI and the diagram in Fig. 14 and Table VII, respectively.

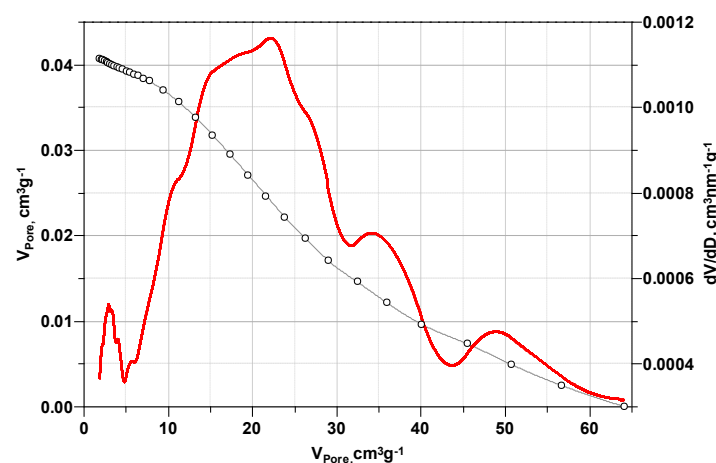


Fig. 11. Active microalloyed ceramics meso pores volume determined by Dollimore and Heal method.

Tab. IV Working conditions and pores examination results obtained by Dollimore and Heal method.

| Working conditions | Value |
|------------------------------------|-------------|
| Linear regression p/p_0 | 0.16 - 0.97 |
| Liquid density / $g\ cm^{-3}$ | 0,8086 |
| Surface voltage / $Dyne\ cm^{-1}$ | 8.85 |
| Results | |
| Mean pore diameter / nm | 25.514 |
| Maximum pore diameter / nm | 22.128 |
| Total pore volume / $cm^3\ g^{-1}$ | 0.0407 |
| Total pore area / $m^2\ g^{-1}$ | 9.147 |

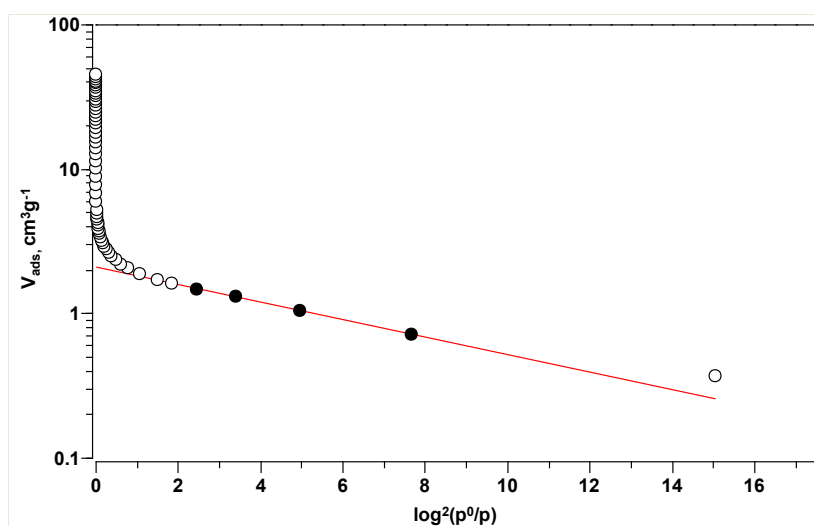


Fig. 12. Active microalloyed ceramics micro pores volume determined by Dubinin and Radaskevich method.

The results which had been obtained using the above test methods confirmed that active microalloyed ceramics had a very developed specific surface in a compact solid state,

in the form of tablets and cylinders, regardless of the fact that many different methods of liquid nitrogen adsorption were used.

Tab. V Working conditions and pores examination results obtained by Dubinin-Raduskevich method.

| Working conditions | Value |
|---|-----------------------------|
| Linear regression $\log^2(p^0/p)$ | 2.174 - 14.31 |
| Alignment | $0.32125666 \pm 0.00373035$ |
| Slope | $-0.0604571 \pm 0.00074232$ |
| r^2 | 0.9998493 |
| Results | |
| Monolayer volume / $\text{cm}^3 \text{g}^{-1}$ | 2.0954 |
| Monolayer content / mmol g^{-1} | 0.0935 |
| Micropores volume / $\text{cm}^3 \text{g}^{-1}$ | 0.0032 |
| Area by Kaganer / $\text{m}^2 \text{g}^{-1}$ | 9.1203 |

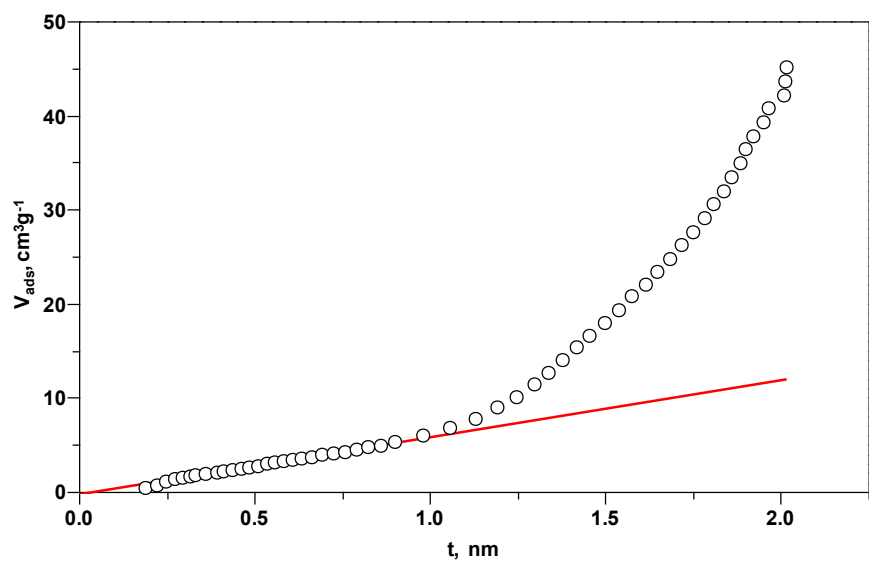


Fig. 13. t-grafic of active microalloyed ceramics monolayer adsorption by Lippens and de Boer method.

Tab. VI Working conditions and micro pores examination results obtained by Lippens-de Boer-a method.

| Working conditions | Value |
|---|-----------------------------|
| Linear regression t / nm | 0.317 - 0.813 |
| Alignment | -0.3103569 ± 0.0050188 |
| Slope | $6.06175253 \pm 0.00882303$ |
| r^2 | 0.99998305 |
| Result | |
| Total area / $\text{m}^2 \text{g}^{-1}$ | 9.3402 |

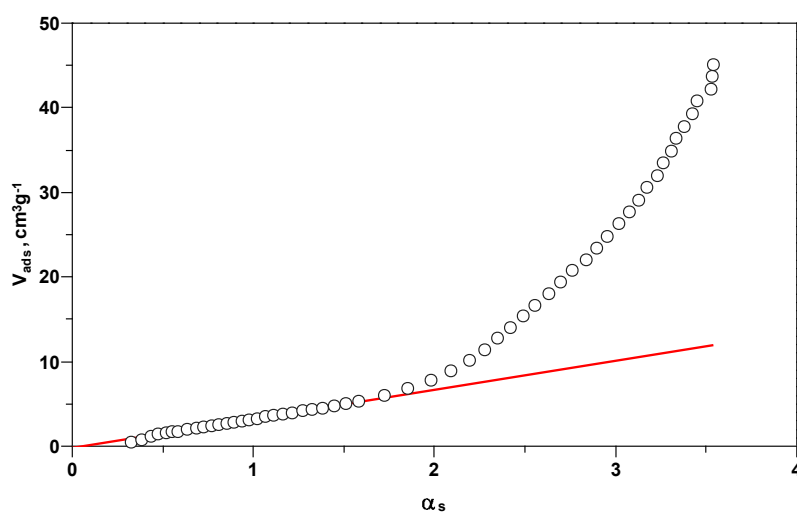


Fig. 14. α -graphic of active microalloyed ceramics surface adsorption by Sing method.

Tab. VII Working conditions and pores examination results obtained by Sing method.

| Working conditions | Value |
|--|-----------------------------|
| Linear regression α_s | 0.554 -1.391 |
| Alignment | $-0.3086715 \pm 0.00452669$ |
| Slope | $3.44828794 \pm 0.00461345$ |
| r^2 | 0.99998479 |
| Result | |
| Total area / m^2g^{-1} | 10.949 |

Thus, determination of porosity and specific surface area confirmed the presence of structural changes in synthesis and sintering process of active microalloyed ceramics. The presented results and obtained parameters indicated that methods for determining pore volume and specific surface area of porous materials depended on the adsorption measurements. Adsorption isotherm accounted for the change in adsorbed nitrogen amount with relative pressure and provided data on pore volume, as shown in Fig. 7.

Specific surface area was determined by Bruner-Emet-Teler method, which was based on physical adsorption of nitrogen monolayer at low temperatures (Fig. 8). Obtained value for specific surface area was $8.6 \text{ m}^2/\text{g}$. Distribution of meso pores was determined by Beret-Joyner-Halend method (Fig. 10). Cumulative pore area of $12.63 \text{ m}^2/\text{g}$ was obtained, and mean pore diameter was 20.3 nm . Distribution of micro pores was determined by Dubinin Raduskevich method (Fig. 12). Specific area (according to Kaganer) was $9.12 \text{ m}^2/\text{g}$. These methods confirmed that active microalloyed ceramics of primary microstructure had a specific structure, with a large number of macro, meso and micro pores and a developed specific surface area.

Thus, the results on pore dimensions on the order of few tens of nanometer, as well as specific surface area of approximately $10 \text{ m}^2/\text{g}$ showed that microalloyed ceramics had a significantly developed surface area and porosity, regardless of the influence of sintering parameters. Despite the fact that it was not possible to determine the dimensions of micro pores due to the capillary Kelvin effect, using existing and world-famous methods, it was certain that micro pores played a very important role in almost all interaction processes and occurred in intergranular space with a fractal nature.

3. Results and Discussion

Thin metal nanostructured films and clusters of newly deposited metals condition channel conductivity of otherwise dielectric materials and changes in numerous structurally sensitive properties. The results are original and unique in world literature and other sources, because such principle (or even a similar one) has not been applied anywhere. Synergistic effect of dislocations and impurities, high temperature and pressures at the sub-grain and grain boundaries, and in the pores play crucial role in the modification of crystal structures and enable dislocation displacement, crystal fragmentation and formation of macro and micro dendritic structures with fractal nature. Further fragmentation is stopped after the formation of mosaic blocks which have a genetically determined crystal structure of the dominant crystal lattice.

The complex multiphase composition of microalloyed ceramics, amorphousness, macro and micro crystallinity, porosity, presence of microalloying and alloying elements and impurities, interfacial contacts and contacts between micro and macro grains are so complex that the intergranular or intergranular space, as well as the developed interfacial space account for numerous processes and interactions of microalloyed ceramics. In addition, due to the contact of dispersed solid phases and permanent change of the dispersion, there is an accumulation of dislocations (helical and linear), which represent the main driving force of the further process and permanent crystal fragmentation. Due to the constancy of this fragmentation process, there are significant changes in micromorphology, structure and all structurally sensitive properties. Of course, when there is annihilation in dislocations movement, mosaic blocks of ideal genetic structure of a certain material appear in an almost completely amorphous structure.

Starting from a fine powder of alumo-silicate clay with dispersed particles not exceeding the dimensions of 0.3-0.5 μm , where all particles originate from agglomerated colloidal particles, the material having a fractal nature has been sintered. Since this material is a matrix for the synthesis and sintering of microalloyed active ceramics with the addition of additives of aluminum, magnesium and other auxiliary materials, it is interesting to explain what happens with starting grains of the matrix during the synthesis and sintering process. It is certain that the fractal nature of alumo-silicate clay, as a granular material, will significantly affect the properties of sintered material. Granular material of alumo-silicate matrix, additives, sodium silicates, water and other modifiers, after sintering, has a complicated, irregular and heterogeneous multiphase microstructure and, above all, a fractal nature. Thus, the fractal nature has much in common with the properties of complex structure and microstructure of active microalloyed ceramics which has been obtained in this manner. In such complex microstructures, where microphases in the form of metal, oxide and silicate films of magnesium and aluminum are layered and deposited on alumo-silicate matrix, very interesting structures of a multiphase heterogeneous solid-solid system are created. Therefore, there is a contact boundary between individual phases, because in addition to intergranular contact boundary of primary microstructure, there is a cluster microstructure, meso and micro pores, defects and dislocations at the matrix grain boundaries-grain contour and at the contact between grains. Consequently, there is a good reason why intergranular surface and volume are considered as admixture and dislocation space, as well as space for accommodation and positioning of very dispersed new phases. This intergranular space is a place where numerous processes of interaction between individual phases take place and where new boundaries and even finer intergranular spaces between nanostructured phases are created.

In active microalloyed alumo-silicate ceramics, there is macro cohesion of multiphase solid material, and for macro and micro grains, in addition to cohesive forces, to maintain the contact boundary between phases and micro-intergranular space, there are charges between interfaces by static electricity. Consistency between microphases is maintained by migratory displacements of polar dielectric ions due to dielectric polarization, microgalvanic couplings

and non-equipotential interfaces. It is certain that nothing can prevent the diffusion and movement of mass along the contours of grains and micro grains, as well as their redistribution. Also, from the originally created cluster microstructures in intergranular space, there is a process of coalescence and their unification into very thin nanostructured films of metal additives Al and Mg, their oxides and nonstoichiometric silicates Mg and Al with a matrix.

It is important to emphasize that the results for specific surface values are incomparably lower than for known highly dispersed and powdered materials, such as activated carbon-based materials and nanomaterials. However, active microalloyed ceramics are destined to be in the form of solid tablets, grains or granules, measuring 10 mm or more, while being compact, solid and mechanically stable. In this state, active microalloyed ceramics can be a multifunctional material, intended for interaction in the solid-liquid and solid-gas system [3,5,10,16,17-23].

4. Conclusion

Based on the presentation and analysis of obtained results, as well as comprehensive discussion of the results, numerous conclusions of a practical and theoretical nature have been made. New technologies cannot be applied unless there are original and innovative materials. For the above stated reasons, active microalloyed alumo-silicate ceramics represents a tremendous challenge for future research, and the research conducted in this paper is only the starting point which has made a certain contribution to the development in this scientific field. Active microalloyed ceramics, as a solid-solid multiphase system, has a dominant amorphous microstructure and micromorphology, a very complex intergranular and interfacial space, where numerous processes and interactions between individual phases take place, create new boundaries and even more complex interfacial spaces between nanostructured phases, and develop microporosity. In multifunctional ceramics, microalloying, alloying and depositing subthin monolayer and multilayer films and Al and Mg films on macro, meso and micro pores and crystal grains of alumo-silicate matrix enable the formation of inhomogeneous and cluster nanostructures. In addition to intergranular contact boundary on grains of alumo-silicate matrix of primary microstructure, there are also boundaries between newly formed phases and on contact between the grains, with cluster nanostructure, meso and micro pores, defects and dislocations. The state of cluster structures is very active, because they are active centers from which electrons are injected through other active centers, where Schottky's above-barrier electron emission applies. Frenkel-Pull effect applies in cases when the distance between clusters and ionizing centers is greater than 40 nm. Aside from cohesion forces, the charge of intermediate surface by static electricity is very important for maintaining micro and macro cohesion of a multiphase system. If the number of macro pores decreases, the number of mezzo pores increases, and eventually, the meso pores are partially transformed into micro pores. Macro and meso pores are formed by the interaction between particles, while micro pores are formed in the interlayer space of alumo-silicate matrix. In active microalloyed ceramics there is macro cohesion of multiphase solid material, and for micro and sub micro grains, in addition to cohesion forces, to maintain the contact boundary between phases and micro-intergranular space, there are charges of interfaces by static electricity.

Acknowledgments

This research is a part of investigations performed within the scope of the project 451-03-68/2022-14/200132. The authors gratefully acknowledge the financial support of Serbian Ministry of Education, Science and Technological Development.

5. References

1. V. S. Cvetković, J. M. Purenović, M. M. Purenović, J. N. Jovićević, Interaction of Mg-enriched kaolinite-bentonite ceramics with arsenic aqueous solutions. *Desalination*, 249 (2) (2009) 582-590.
2. M. Ranđelović, M. Purenović, A. Zarubica, J. Purenović, I. Mladenović, G. Nikolić, Alumosilicate ceramics based composite microalloyed by Sn: an interaction with ionic and colloidal forms of Mn in synthetic water. *Desalination*, 279 (1-3) (2011) 353-358.
3. J. Purenović, V. V. Mitić, V. Paunović, M. Purenović, Microstructure characterization of porous microalloyed aluminium-silicate ceramics. *Journal of Mining and Metallurgy, Section B: Metallurgy*, 47 (2) B (2011) 157-169.
4. M. Ranđelović, M. Purenović, A. Zarubica, J. Purenović, B. Matović, M. Momčilović, Synthesis of composite by application of mixed Fe, Mg (hydr) oxides coatings onto bentonite - a use for the removal of Pb(II) from water. *Journal of Hazardous Materials*, 199-200 (2012) 367-374.
5. J. Purenović, V. V. Mitić, Lj. Kocić, V. Pavlović, V. Paunović, M. Purenović, Electrical properties and microstructure fractal analysis of magnesium-modified aluminium-silicate ceramics. *Science of Sintering*, 43 (2) (2011) 193-204.
6. M. Ranđelović, M. Purenović, J. Purenović, Physico-chemical interaction between microalloyed and structurally modified composite ceramics and sulphide solutions. *Journal of Environmental Protection and Ecology*, 11 (4) (2010) 1446-1457.
7. M. Ranđelović, M. Purenović, A. Zarubica, I. Mladenović, J. Purenović, M. Momčilović, Fizičko-hemijska karakterizacija bentonita i njegova primena u uklanjanju Mn^{2+} iz vode. *Hemijska industrija*, 65 (4) (2011) 381-387.
8. M. Ranđelović, M. Purenović, J. Purenović, Effect of immobilised thin layers of organic matter on Mn^{2+} removal from water systems by bentonite composite. *Journal of Environmental Protection and Ecology*, 12 (3) (2011) 1049-1057.
9. M. Ranđelović, M. Purenović, J. Purenović, M. Momčilović, Removal of Mn^{2+} from water by bentonite coated with immobilized thin layers of natural organic matter. *Journal of Water Supply: Research and Technology – AQUA*, 60 (8) (2012) 486-493.
10. Jelena M. Purenović (2009). Microstructure characteristics and electrical properties of modified alumo-silicate ceramics. *Master's thesis*, Faculty of Electronic Engineering, University of Niš.
11. M. M. Purenović, scientific study, with know-how technology, deposited with the Intellectual Property Office of the Republic of Serbia under number A-641/06/1 from 25.1.2007.
12. K. J. Falconer, The geometry of fractal sets. New York: Cambridge University Press; 1985.
13. Lj. M. Kocić, V. V. Mitić, and M. M. Ristić, Stereological Models Simulation of $BaTiO_3$ -Ceramics Grains, *J. Materials Synthesis and Processing*, 6(5) (1998) 339-344.
14. T. Allen, Particle Size Measurement. Vol. 2: Surface area and pore size determination, Chapman & Hall, London, 1997.
15. T. Allen, Powder Sampling and Particle Size Determination, Elsevier, 2003.

16. J. M. Purenović, Lj. Živković, M. Miljković, SEM and EDS characterization of Mg-activated kaolinite-bentonite ceramics. *Proceeding of the Sixth Students' Meeting-SM-2005, School of Ceramics, Novi Sad, Serbia and Montenegro, December 1-2, 2005*, pp.103-106.
17. J. Purenović, M. Randjelović, B. Matović, M. Purenović, Application of Minkowski layer for intergranular fractal surfaces of multiphase active microalloyed and alloyed aluminium - silicate ceramics. *Applied Surface Science*, 332 (2015) 440-455.
18. Jelena M. Purenović (2013). Electrophysical and fractal microstructural characterization of microalloyed alumo-silicate ceramics. *Doctoral dissertation, Faculty of Electronic Engineering, University of Niš*.
19. M. S. Randjelovic, M. M. Purenović, B. Z. Matović, A. R. Zarubica, M. Z. Momčilović, J. M. Purenović, Structural, textural and adsorption characteristics of bentonite - based composite. *Microporous and Mesoporous Materials*, 195 (2014) 67-74.
20. J. Purenović, V. V. Mitić, Lj. Kocić, V. Pavlović, M. Randelović, M. Purenović, Intergranular area microalloyed aluminium-silicate ceramics fractal analysis. *Science of Sintering*, 45 (1) (2013) 117-126.
21. J. Purenović, V. V. Mitić, M. Randelović, B. Matović, M. Purenović, Electrophysical properties of microalloyed alumo-silicate ceramics as active dielectric. *Serbian Journal of Electrical Engineering*, 10 (1) (2013) 175-184.
22. Jelena Purenović, Microstructural and electrical characteristics of modified alumo-silicate ceramics. *IEEEESTEC-3rd student projects conference, Faculty of Electronic Engineering, Niš, 2010*, pp. 75-79. ISBN: 978-86-6125-021-7.
23. J. Purenović, M. Randelović, B. Matović, M. Purenović, Electrophysical properties of microalloyed alumo-silicate ceramics as an active dielectric. *56th Conference on Electronics, Telecommunications, Computing, Automation and Nuclear Engineering, ETPAN 2012, Zlatibor, 11-14. June 2012*, pp. 60. (First-prize-winning work in the New Materials section)
24. M. Kokunešoski, M. Stanković, M. Vuković, J. Majstorović, Đ. Šaponjić, S. Ilić, A. Šaponjić, Macroporous monoliths based on natural mineral sources, clay and diatomite, *Science of Sintering*, 52 (3) (2020) 339-348.
25. J. J. Sánchez-Cuevas, J. Zárate-Medina, O. Navarro, C. Mercado-Zúñiga, F. J. Reynoso-Marín, G. Rosas, Microstructure and microhardness of the Al-10Mg alloy processed by the mechanical alloying technique, *Science of Sintering*, 52 (2) (2020) 123-133.

Сажетак: Мултифункционална активна микролегирана алумо-силикатна керамика, као сложен вишефазни хетерогени систем у чврстом стању има нехомогену структуру са интергрануларним простором, која се одражава на низ структурно-осетљивих мултифункционалних својстава. Веома сложен интергрануларни простор и бројне интеракције између појединих фаза и зрна стварају нове границе и још сложенији простор са знатно мањим микрозрнима, који су настали фрагментацијом зрна покретањем дислокација. Поред смањења макро и мезо порозности, денсификацијом интергрануларног простора повећава се број микро пора. Интергрануларна површина и запремина сматрају се дислокационим простором. Методом квантитативне металографије извршено је одређивање расподеле величине зрна, користећи софтвер за аутоматску анализу. На посебним узорцима мултифункционалне керамике, извршена су испитивања специфичне површине, као и расподеле пора. Коришћене су стандардне методе одређивања специфичне површине узорака у вакууму. Добијени резултати, релевантни са гледишта теоријске и практичне примене, потврдили су да мултифункционална активна микролегирана

керамика има развијену површину са значајним бројем мезо и микро пора. Услед константности процеса фрагментације зрна, дошло је до значајних промена у микроморфологији и свим мултифункционалним својствима, као и до померања дислокација, што је дало значајан допринос савременим истраживањима у овој области.

Кључне речи: мултифункционална керамика, дистрибуција зрна, макро мезо и микро порозност, дислокација, фрагментација.

© 2023 Authors. Published by association for ETRAN Society. This article is an open access article distributed under the terms and conditions of the Creative Commons — Attribution 4.0 International license (<https://creativecommons.org/licenses/by/4.0/>).

